Natural Resources Canada
Ressources naturelles Canada

# Analysis and reprocessing of the Strange Lake airborne gravity gradiometry survey, Quebec and Newfoundland and Labrador

*P. Keating and M. Pilkington*

**Geological Survey of Canada**
**Current Research 2013-15**

**2013**

Canada

Geological Survey of Canada
Current Research 2013-15


# Analysis and reprocessing of the Strange Lake airborne gravity gradiometry survey, Quebec and Newfoundland and Labrador

*P. Keating and M. Pilkington*

2013

ISSN 1701-4387
Catalogue No. M44-2013/15E-PDF
ISBN 978-1-100-22261-5
doi:10.4095/292569



**Recommended citation**

Keating, P. and Pilkington, M., 2013. Analysis and reprocessing of the Strange Lake airborne gravity gradiometry survey, Quebec and Newfoundland and Labrador; Geological Survey of Canada, Current Research 2013-15, 13 p. doi:10.4095/292569

***Critical review***
*W. Miles*

***Authors***
***P. Keating (Pierre.Keating@NRCan-RNCan.gc.ca)***
***M. Pilkington (Mark.Pilkington@NRCan-RNCan.gc.ca)***
*Geological Survey of Canada*
*615 Booth Street*
*Ottawa, Ontario*
*K1A 0E8*

Correction date:

# Analysis and reprocessing of the Strange Lake airborne gravity gradiometry survey, Quebec and Newfoundland and Labrador

P. Keating and M. Pilkington

Keating, P. and Pilkington, M., 2013. Analysis and reprocessing of the Strange Lake airborne gravity gradiometry survey, Quebec and Newfoundland and Labrador; Geological Survey of Canada, Current Research 2013-15, 13 p. doi: 10.4095/292569

**Abstract:** The high-resolution airborne gravity-gradiometry survey flown in March 2012 over the Strange Lake intrusive complex provides an opportunity to better understand the performance and limitations of this technology and also investigate potential improvements to the associated data processing. To this end, gravity-gradient data low-pass filtered at 75 m, rather than the standard 300 m, was provided by the contractor. Repeated flights along a single line were used to assess the repeatability of the data and it was found that in this particular area the airborne gradient-gravity system has a full sine (wavelength) resolution of about 700 m. The system can therefore detect anomalies having a width of about 350 m. We found that for this type of data, kriging is a better interpolator than low-pass filtering combined with minimum curvature gridding. Using kriging, the line-to-line correlation, and in some cases the resolution, appears slightly improved.

**Résumé :** Le levé aérien de gradio-gravimétrie à haute résolution, effectué en mars 2012 au-dessus du complexe intrusif de Strange Lake, donne l'occasion de mieux comprendre le rendement et les limites de cette technologie et également d'étudier des améliorations possibles du traitement des données obtenues. À cette fin, l'entrepreneur a fourni les données du gradient de gravité soumises à un filtrage passe-bas à 75 m, plutôt qu'à la valeur habituelle de 300 m. Des vols répétés le long d'une seule ligne ont permis d'évaluer la répétabilité des données et il a été constaté que, dans cette zone particulière, le système de gradio-gravimétrie aéroporté a une résolution d'une longueur d'onde sinusoïdale complète d'environ 700 m. Ainsi, le système permet de détecter des anomalies d'une largeur d'environ 350 m. Nous avons constaté que, pour ce type de données, le krigeage est une meilleure méthode d'interpolation que le filtrage passe-bas combiné à un quadrillage de la courbure minimale. La corrélation d'une ligne à une autre est améliorée et, dans certains cas, la résolution est légèrement plus élevée.

## INTRODUCTION

An airborne combined gravity-gradiometric and magnetic survey was flown over an area immediately east of Lake Brisson, about 235 km northeast of Schefferville, Québec and 125 km west of Voisey's Bay, Newfoundland and Labrador (Fig. 1). The survey is centred on the Strange Lake peralkaline granite (Miller, 1990; Pillet et al., 1992) that hosts a rare-earth metal deposit known as the Strange Lake deposit. The objective of the airborne gravity-gradiometry survey was to map the internal structure of the Strange Lake intrusive complex.

The intrusive is subcircular and consists of generally concentric, high-level granitic intrusions bounded by sharp contacts with country rocks. It is thought to be related to the Mistastin Batholith. Ring faults, at or near the contact of the alkalic complex, dip outward at low to moderate angles (20°–35°). A small stock of medium-grained, generally nonporphyritic 'exotic-rich' granite with very high overall values of zirconium, niobium, yttrium, and rare-earth elements (REE) is located at the centre of the complex (Miller, 1990). The Strange Lake deposit is located on the west shore of Lake Brisson along the western limit of the intrusive complex.

A similar gravity-gradiometric survey, at a line spacing of 250 m, was flown in 2011 over the McFaulds Lake area in northern Ontario. A major chromite deposit and small volcanogenic massive-sulphide deposits are located within the area. Although the survey could not detect specific deposits, it was useful for geological mapping and helped provide a better understanding of the geology of the area (Rainsford et al., 2011). Because of the success of this survey, it was decided to fly the Strange Lake area at a tighter line spacing to test the limits of the technology. The initial intent was to try to map the internal structure of the intrusive complex, but the acquired gravity-gradiometry data now indicate that the density contrasts, if present, are too weak to characterize any internal variations within the intrusive complex.

Due to the experimental nature of this survey, additional data were acquired by the contractor. Firstly, an east-west line was flown five times to investigate the repeatability of the results and the noise level of the data. Secondly, 20 east-west lines were flown halfway between 100 m spaced lines to determine if the resolution of the system could be increased by flying at a tighter line spacing. Also, 20 repeat lines, i.e. lines flown twice, were flown in this area, but they were not used in the current study. This gives a series of lines at a 50 m interval. The location of these 40 lines was selected to pass over the Strange Lake deposit. After completion of the survey it was realized that the Strange Lake complex does

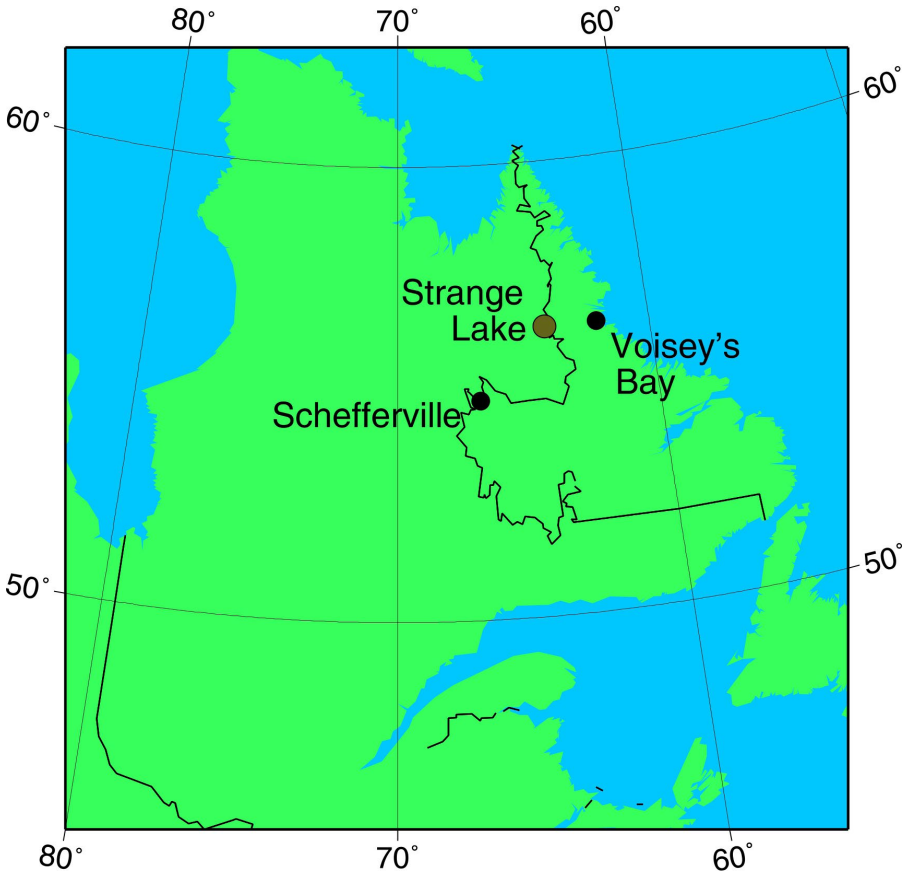


**Figure 1.** Location map of the survey area.

not show any well defined internal structure, either in the gravity data or the magnetic data, and that additional work was required to understand the geophysical data.

The Falcon™ system used to acquire the airborne gravity-gradient data are derived from an instrument developed for the U.S. Navy during the Cold War. The technology was later allowed to be used for civilian applications. It nevertheless remains subject to International Traffic in Arms Regulations (ITAR) restrictions from the U.S. government. In practise, this means that access to the raw data is restricted and that the raw data cannot be published. Figure 2 shows the three orthogonal components of the gravity field and the tensor components that are determined from the survey data. The co-ordinate axes are North (N), East (E) and Down (D). The tensor components are simply the three orthogonal gradients, or rate of change, of each one of the components. Gravity is a potential field and obeys Laplace's equation. Therefore the sum of the diagonal elements of the tensor is zero ($G_{EE}+G_{NN}+G_{DD} = 0$). The tensor is also symmetric: $G_{NE} = G_{EN}$, $G_{ND} = G_{DN}$ and $G_{ED} = G_{DE}$. There are therefore only five independent components. The Falcon™ system measures the horizontal curvatures $G_{UV}$ and $G_{NE}$ of the gravity field and the components of the gradient gravity tensor are calculated from these two measurements; $G_{UV}$ being equal to $(G_{NN}-G_{EE})/2$.

## SURVEY

The survey was flown by Fugro Airborne Surveys (FAS) from March 13, 2012 to April 8, 2012. East-west oriented flight lines, spaced 100 m apart were flown at a nominal terrain clearance of 80 m. Control lines were flown north-south at an interval of 1200 m. Differential GPS was used for navigation and flight path recovery. Location accuracy is 3 m or better. A LiDAR system was used to obtain a digital elevation model (DEM) of the survey area; this DEM was later used to compute topographic corrections for the gravity data. A Falcon™ Airborne Gradient Gravity (AGG) system (Dransfield, 2007) was used to obtain the vertical gradient of gravity. The curvature components are demodulated, corrected for aircraft motion and low-pass filtered along line with a six-pole Butterworth filter with a cut-off frequency of 0.18 Hz or about 300 m (Dumont and Jones, 2012). Other cut-off wavelengths could also be used to attempt producing higher spatial resolution but noisier data. The 300 m cut-off wavelength was determined by trial and error by FAS. Topographic corrections were calculated for the curvature components ($G_{UV}$ and $G_{NE}$) up to a distance of 10 km from the measurement points. The LiDAR-derived DEM is used inside the survey area and the Shuttle Radar Topographic Mission derived DEM is used outside the survey area. A density of 2670 kg/m$^3$ was used to compute the topographic

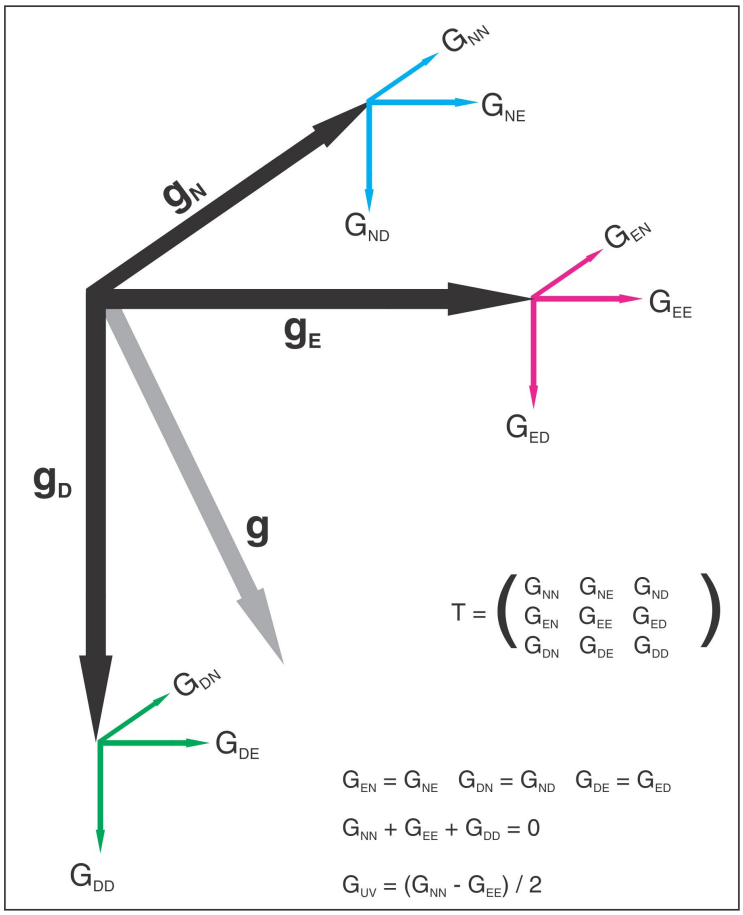


**Figure 2.** The gravity tensor T. The tensor matrix and the relationships between its components are shown: E: East. N: North, D: Down.

corrections. This density minimizes the correlation between the topography and the corrected vertical gravity gradient. The two corrected curvature components of the gravity tensor were levelled using least-squares minimization of the differences at survey line intersections.

All tensor components, corrected for topography, are calculated by Fast Fourier Transform. Equivalent sources can also be used to calculate $g_D$, $G_{DD}$, $G_{NE}$, and $G_{UV}$. Both methods were used by the contractor and provide very similar results. From a geological mapping perspective $G_{DD}$, the vertical gradient of the gravity field and $g_D$, the vertical component of gravity, which is equivalent to the usual Bouguer anomaly, are the most useful data.

## GRAVITY AND MAGNETIC MAPS

Maps of the published vertical component of gravity ($g_D$) and its vertical gradient ($G_{DD}$) are presented in Figure 3a and b; these maps were produced from data low-pass filtered with a standard 300 m cut-off wavelength. The residual total magnetic field and its first vertical derivative are shown in Figure 4a and b. There is no obvious signature of the Strange Lake complex or the REE deposit in $g_D$ or $G_{DD}$. In the northern part of the survey area north-northwest-oriented gravity-gradient anomalies are associated, along with magnetic anomalies, with bands of gneisses and paragneisses mapped by Bélanger (1984). The eastern part of the area also contains many gneissic bands, but they have a weaker gravity-gradient signature. Elsewhere, the vertical gradient of gravity does not show coherent patterns that may be related to geological sources. The DEM for the survey area is shown in Figure 5. A few east-northeast-trending gravity-gradient anomalies correlate with the topography indicating an incomplete topographic correction. Some of the east-northeast-trending topographic features are sand and gravel deposits left after the last glaciation. They likely have a density of 2.2 g/cc, lower than the density of 2.67 g/cc used for the topographic corrections.

The vertical component of gravity, $g_{D,}$ is calculated by vertically integrating $G_{DD}$ (Blakely, 1996). The Falcon™ system cannot measure the long wavelength components of the gravity field. These can be recovered by conforming $g_D$ to the regional gravity field obtained from the Canadian National Gravity Data Base (Dransfield, 2010a). Gravity stations used for this purpose have a spacing between 7 km and 9 km in the area. There are three stations within the survey area and two along the edges.

## ANALYSIS

### Profile data

Figure 6a shows a profile of vertical gravity-gradient data from line 11220 located in the northern part of the survey (location given in Figure 6c). A detailed zoom of the central part of the profile is shown in Figure 6b. This line was chosen since it intersects (431000E) a strong vertical gravity-gradient anomaly that has amplitude of about 80 E. Corrected data obtained after applying a Butterworth filter with cut-off wavelengths of 75 m, 100 m, 150 m, and 300 m are shown. A cleaner signal is obtained as the cut-off wavelength increases. The published vertical gravity gradient (Dumont and Jones, 2012) shown in Figure 3b is from the 300 m low-pass filtered data. In an attempt to improve upon the resolution provided by the data in Figure 3b, a grid of the 75 m low-pass filtered vertical gradient-gravity data was interpolated at a grid cell of 25 m by minimum curvature (Fig. 6c). Unfortunately it shows little correlation between data from adjacent flight lines except over the gneissic units in the northern part of the map. To the south, the map is dominated by short-wavelength, high-amplitude noise making it of little use for geological mapping.

### Profile spectra and coherence

The repeated flight line flown in the northern part of the survey (located in Figure 9a) allows us to estimate the repeatability of the data as well as to estimate their resolution. Resolution of the data is often estimated by measuring the width of the narrowest anomalies that are coherent, or repeated, over adjacent lines. This width corresponds to the half-sine (half-wavelength) resolution of the data. The full-sine resolution is twice this width. This is because widths are generally measured between the inflection points of an anomaly or between the zero contours on both sides of a maximum in the case of a gradient anomaly. In the case of the Strange Lake survey the visually estimated width of the narrowest anomalies is about 300 m corresponding to a full sine resolution of 600 m.

A quantitative estimate of the resolution of the data can be obtained by computing the coherence (Kanasewich, 1981) between the vertical gravity gradient from two of the repeated flights (1093500–7 and 1093500–5) using the 75 m low-pass filtered data. Figure 7a shows the energy spectra of these two flights and their coherence. Falcon™ data processing is grid-based (Dransfield et al., 2001) rather than line-based as for aeromagnetic data. Line data are therefore values extracted from the processed grid. In the present case, the average sampling interval of the line data was about 7 m, but the grid interval was 25 m. The shortest wavelength (Nyquist frequency) is therefore 50 m. Both energy spectra are nearly identical and decay rapidly at wavelengths smaller

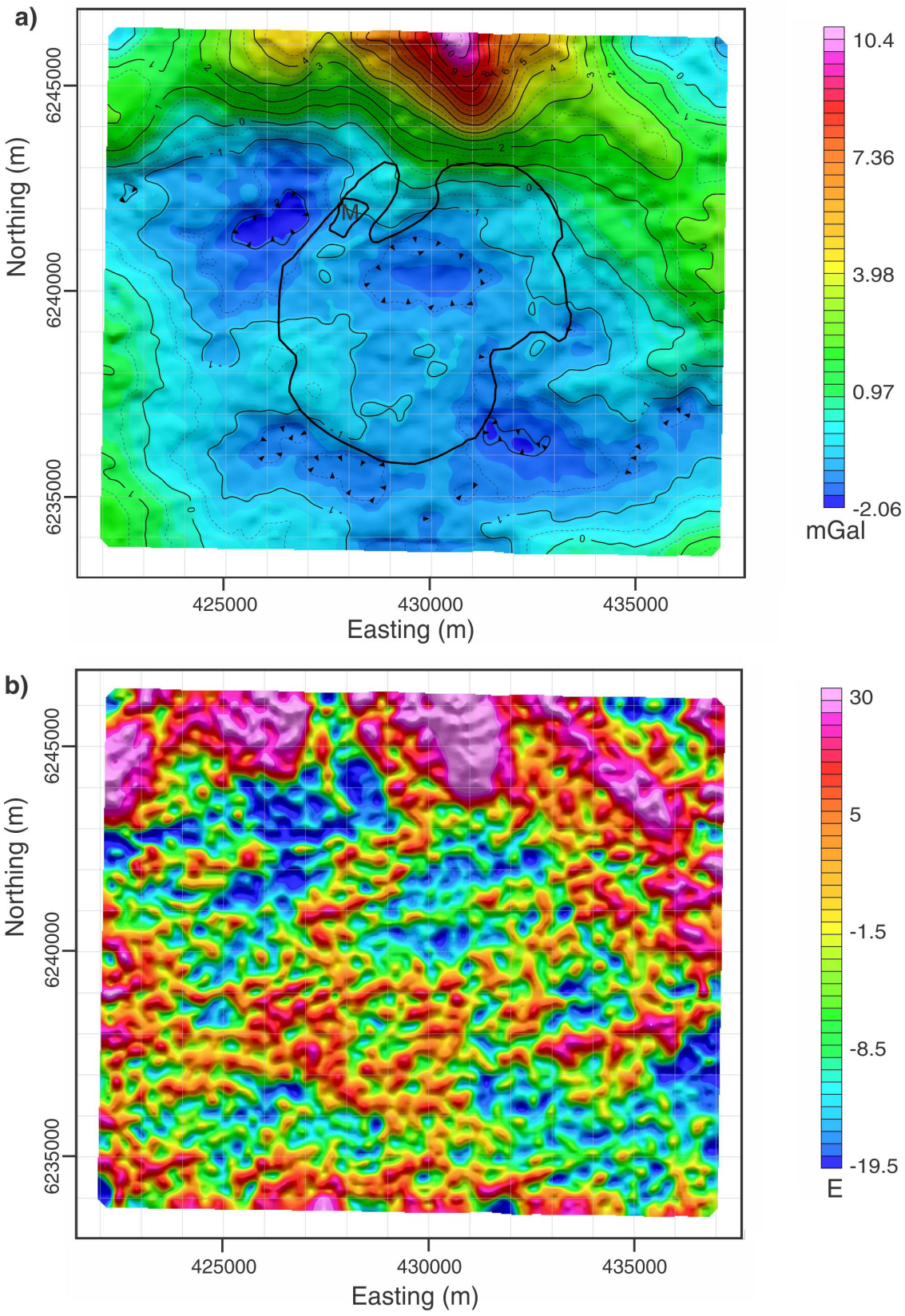


**Figure 3. a)** Vertical component of the gravity field in the Strange Lake area. The black line outlines the Strange Lake intrusive complex. M denotes mineralized zone. **b)** Vertical gradient of the gravity field in the Strange Lake area.

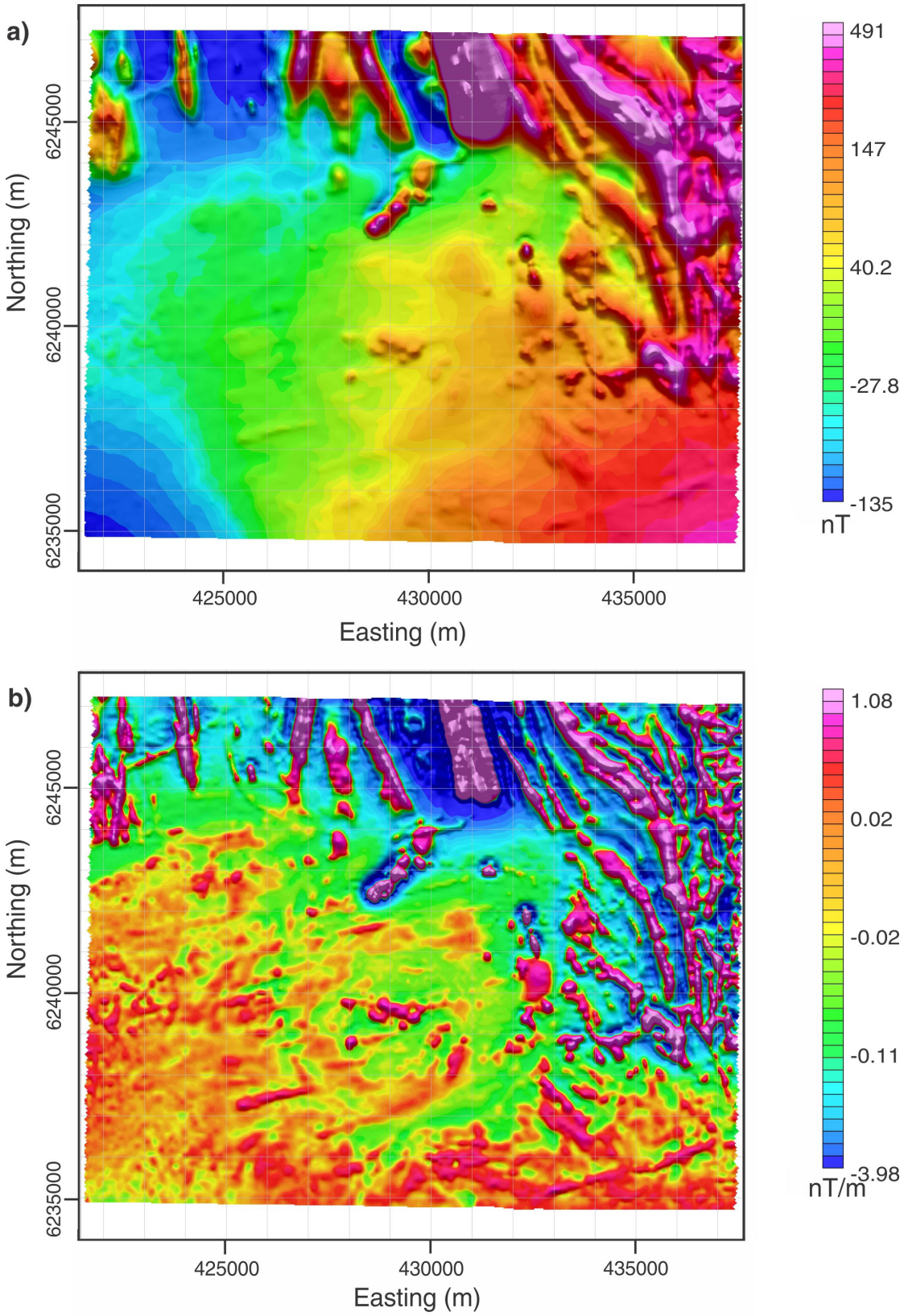


**Figure 4. a)** Residual total magnetic field in the Strange Lake area. **b)** First vertical derivative of the magnetic field in the Strange Lake area.

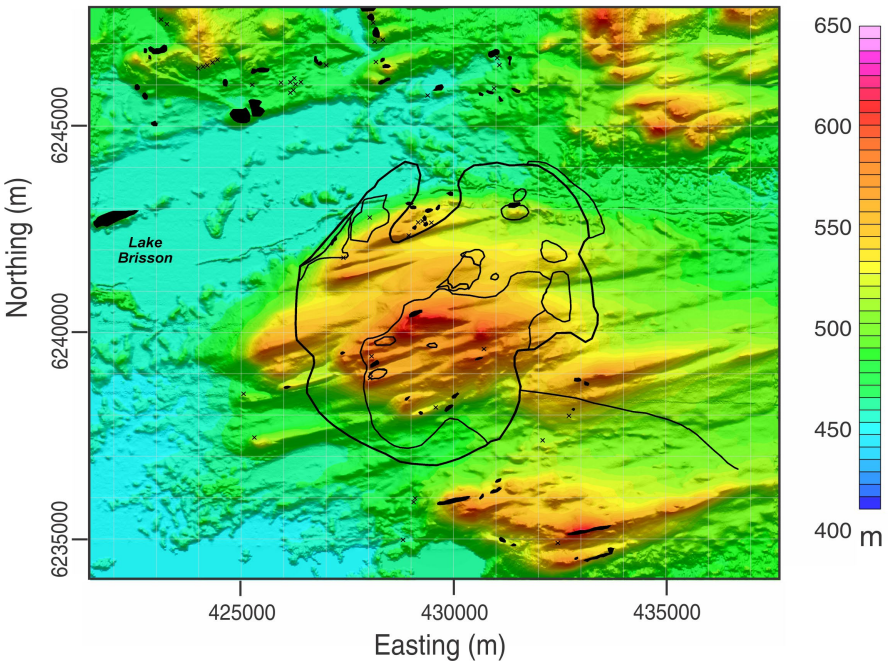


**Figure 5.** Digital elevation model from LIDAR and SRTM data. Black lines are major geological contacts. Crosses indicate outcrops and black areas are large outcrops. Geology adapted from Bélanger (1984) and Miller (1990).

than 100 m. Between 100 m and Nyquist the power drops by 6 orders of magnitude indicating that there is almost no signal at wavelengths smaller than ~70 m.

The coherence (Fig. 7b) drops to 0.5 (the transition from coherent to incoherent signal) at a wavelength of 700 m. Even if the frequency content of both flights is similar at wavelengths smaller than 700 m, the coherence indicates that the signals from both lines are not in phase. This means that anomalies shorter than 700 m are likely due to noise. This matches the estimate from visual observations. This should not be interpreted as meaning that the full-sine resolution of the Falcon™ system is 700 m; rather it means that data from this specific line has a resolution of 700 m. This is simply because there are no shorter wavelength anomalies standing out above the noise level.

## REPROCESSING

Filtering the gravity-gradiometry data using frequency-domain filters with different cut-off wavelengths will not improve the line-to-line continuity as these filtering tests have already been done by FAS as part of their routine processing stream. Ideally, we would like to use an estimator that improves the continuity of the data and that adapts locally to the characteristics of the line data. Here we propose to use a statistical technique known as kriging to estimate the best vertical gravity-gradient values ($G_{DD}$) at any location within the survey area. The same procedure could be used for the other tensor components, but we prefer to use $G_{DD}$ as it is the one most commonly used for geological mapping. Kriging can be seen as a form of moving average driven by the spatial distribution of the data and their statistical properties. Kriging assumes that data are randomly distributed in space. The statistical character of the data is empirically described by the variogram which measures the variance of the data as a function of distance and direction (Isaaks and Srivastava, 1989; Deutsch and Journel, 1992). The variogram is calculated from the squared differences of all data pairs within the gridding area. Data points located close to each other are expected to have almost the same values; differences are due to noise, slightly different locations, and measurement errors. Points located far away from each other are not expected to have similar values, i.e. they are less correlated than closely spaced values. In general, the variogram is an increasing function of distance (Chilès and Delfiner, 1999). At very short distances it is characterized by the nugget effect (nonzero variance) which, in the present case, mostly corresponds to the noise level of the data.

Before kriging of data values, a model has to be fitted to the variogram. For the Strange Lake data we fitted an isotropic exponential model. Selecting an isotropic model ensures that no directional bias will be introduced. The variogram and the model are shown in Figure 8. The value of the nugget effect is 280 $E^2$, which implies a noise level of 16.7 E. This is much greater than the published 6 E instrumental noise for the Falcon™ system but it also includes other sources of noise: imperfect corrections and data aliasing in the direction perpendicular to the flight-line orientation. It is therefore an upper bound on the data noise. Once the variogram model is specified, it is used as the basis for the interpolation of the line data onto a regularly spaced grid.

The vertical gradient of the gravity ($G_{DD}$) interpolated by kriging the 75 m low-pass filtered data are shown in Figure 9a. Visually the map shows better line-to-line continuity than

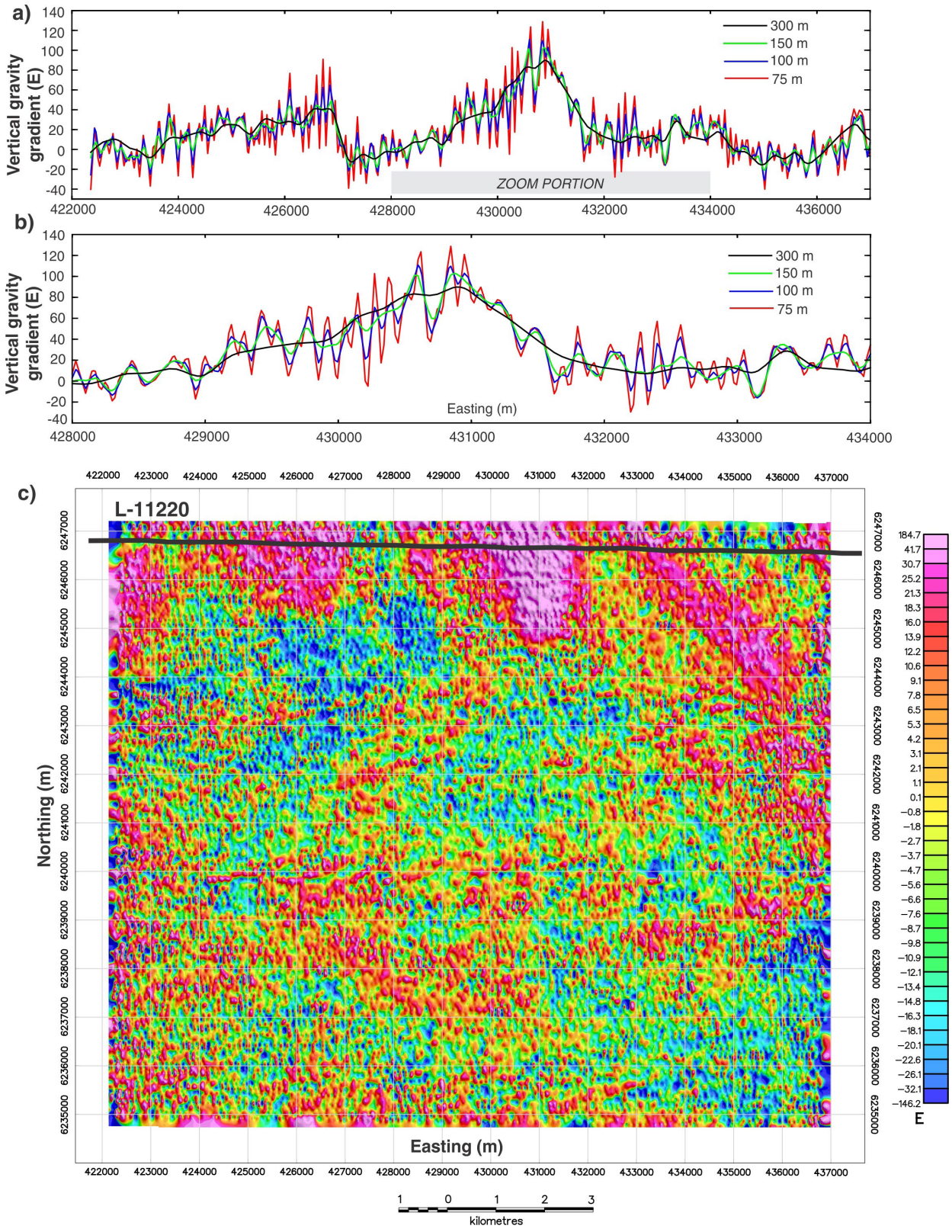


**Figure 6. a)** Vertical gravity gradient from line 11220 for different cut-off wavelengths. **b)** Detail of portion of line 11220. **c)** Vertical gravity gradient map from the 75 m low-pass filtered data. Grid cell is 25 m. The black line indicates the location of line 11220.

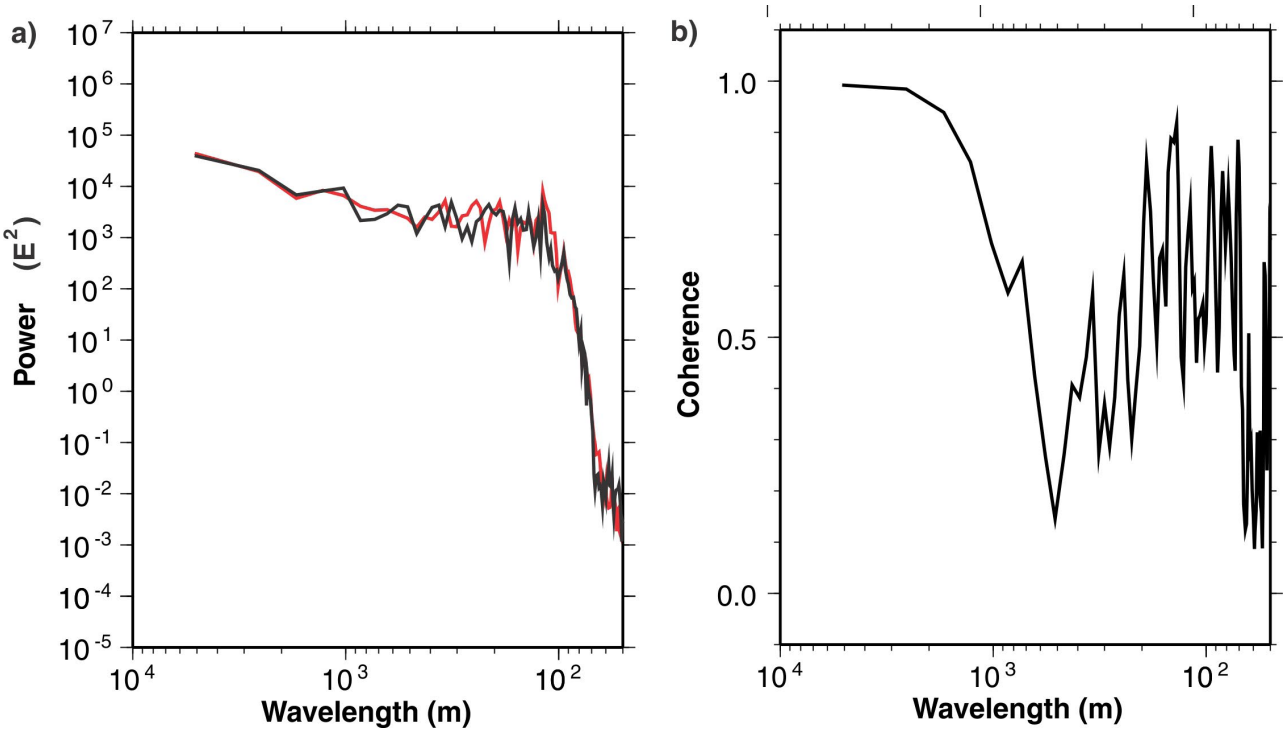


**Figure 7. a)** Spectra of $G_{DD}$ for two of the repeat flights. Their location is shown in Figure 9a. **b)** Coherence between $G_{DD}$ from the same two lines.

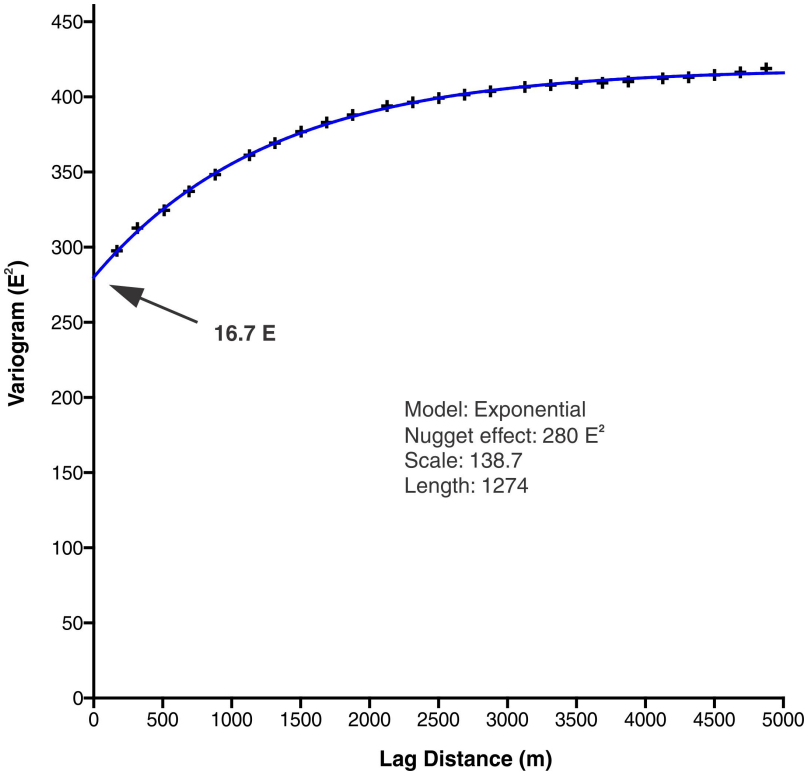


**Figure 8.** Variogram of the 75 m low-pass filtered vertical gravity-gradient data. Lag distance is the distance between each pair of data values. Crosses are calculated and the blue line is the fitted exponential model. Model parameters are given in the figure.

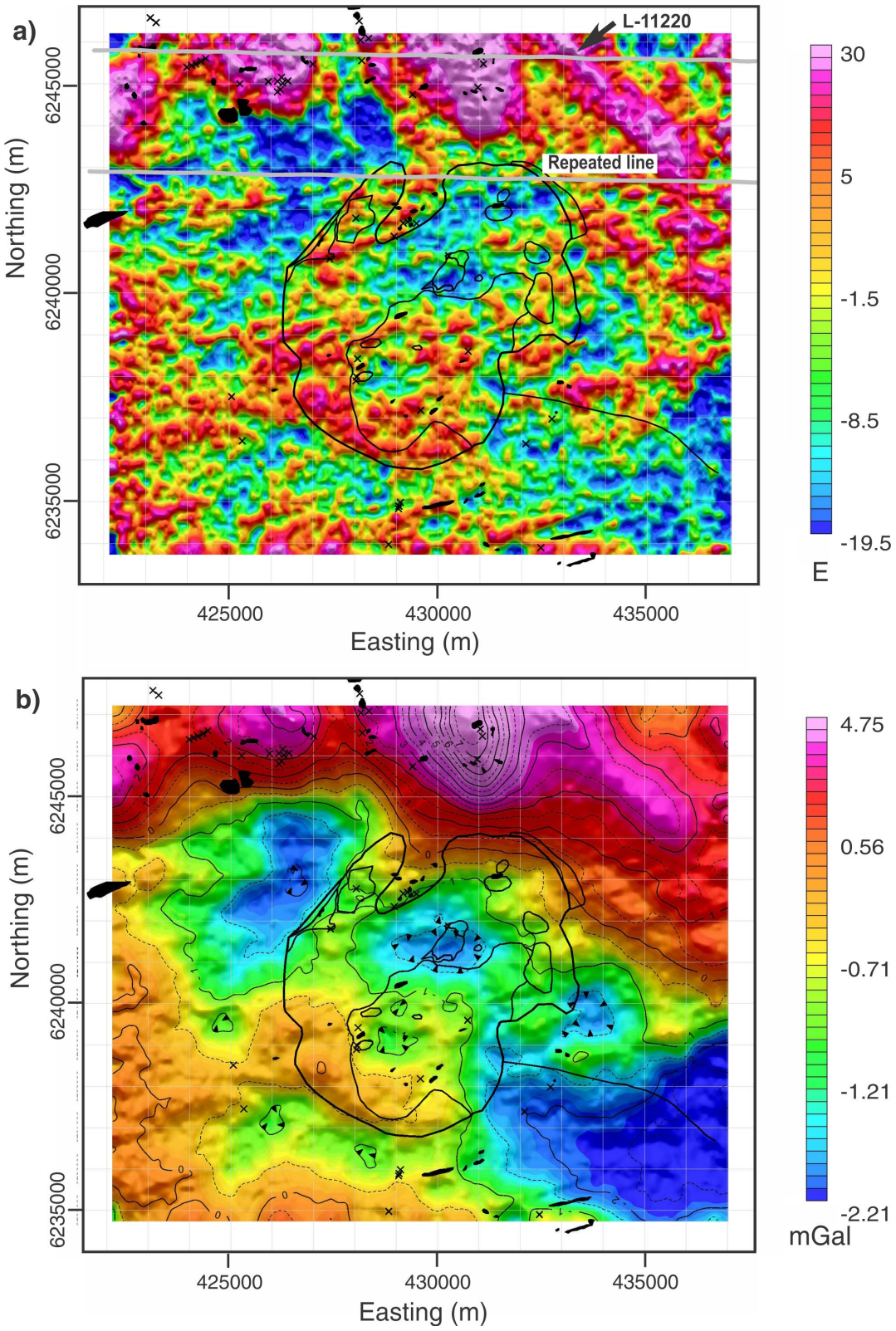


**Figure 9. a)** Vertical gradient of the gravity calculated by kriging the 75 m low-pass filtered data. **b)** Vertical component of the gravity field calculated by vertically integration the vertical gradient of the gravity calculated by kriging the 75 m low-pass filtered data. Grid cell is 25 m. Black lines are major geological contacts. Crosses indicate outcrop and black areas are large outcrops. Geology adapted from Bélanger (1984) and Miller (1990).

the grid obtained from the 300 m low-pass filtered data. This is apparent in a series of east-northeast-trending anomalies that correspond to glacial drift. The amplitude of these anomalies varies between 10 E and 15 E, just above the instrumental noise level. They are much weaker than the anomalies caused by the gneissic units located in the northern part of the map, where amplitudes reach 80 E, well above the noise level. The vertical gradient of the gravity ($G_{DD}$) was vertically integrated to obtain the vertical component of the gravity field ($g_D$) shown in Figure 9b. It was not conformed to the regional gravity grid and is therefore equivalent to a residual gravity map. The gravity low over Lake Brisson is partly caused by an insufficient topographic correction due to the lack of bathymetric data, but it is nevertheless real. Its real amplitude is certainly smaller than shown in Figure 9b.

Figure 10 presents a comparison of vertical gravity-gradient data estimated by kriging the 75 m low-pass filtered data and data from the 300 m low-pass filtered data. This is the same section as shown in Figure 6b along line 11220. The kriged profile contains shorter wavelength details, but it is impossible to know if they are real or not. Nevertheless, the good continuity apparent in Figure 9a suggests that there is useful, reliable signal in the kriged grid (and profile). The coherence estimate from Figure 7b indicates the anomalous features in the kriged profile with wavelengths greater than 350 m (e.g. centred on 429500E, 433750E) are reliable. Nearby the main gradient maximum (430700E), the difference between the two profiles is 6 E, which is within the instrumental noise level of the system.

## Spectra

The radially averaged spectra of the grids (25 m grid cell) calculated from the 75 m and 300 m low-pass filtered data, and the grid calculated by kriging the 75 m low-pass filtered data are shown in Figure 11. Grids of the first two data sets were calculated using minimum curvature (Briggs, 1974). The effects of the cut-off wavelengths are clearly visible in the spectra of the 75 m and 300 m low-pass filtered grids. The long wavelength portion of the energy spectrum of the 75 m low-pass minimum curvature grid decays rapidly for wavelengths longer than 500 m. The decay then slows downs and starts increasing with a small peak at a wavelength of 110 m. The spectrum is then affected by the 75 m low-pass filter and starts decreasing again. At the Nyquist wavelength (50 m) the energy level is still much higher that that of the 300 m low-pass filtered data. This reflects the higher noise level of the 75 m minimum curvature grid. The spectrum of the grid calculated by kriging does not decay as rapidly as that from the 300 m low-pass filtered data, but their energy levels at the Nyquist wavelength are similar. Also, the kriged-grid energy spectrum has more energy at mid wavelengths, but slightly less energy than the 300 m low-pass filtered data grid at around a wavelength of 500 m. This is investigated by computing the difference between these two grids (Fig. 12). The standard deviation of the difference is 3.4 E, less that the quoted 6 E instrumental noise level of the Falcon™ system (Dransfield, 2010b). Long-wavelength east-west trends, having a north-south width between 2 km and 4 km are visible in the difference map. This suggests that these small amplitude trends are associated with some flight line effects. A possible cause is that kriging uses data points from at least 200 m north and 200 m south of any interpolated points and is, on average, using data from five flight lines. On the other hand, minimum curvature is mostly influenced by data points near the interpolated grid cell (Briggs, 1974). The observed differences are likely caused by very small-level changes between flight lines. In any case, these differences are smaller than the instrumental noise level of the system.

# CONCLUSIONS

The along-line resolution of the Strange Lake survey as determined visually and from repeat lines is about 350 m (half-sine resolution). Kriging of the 75 m low-pass filtered

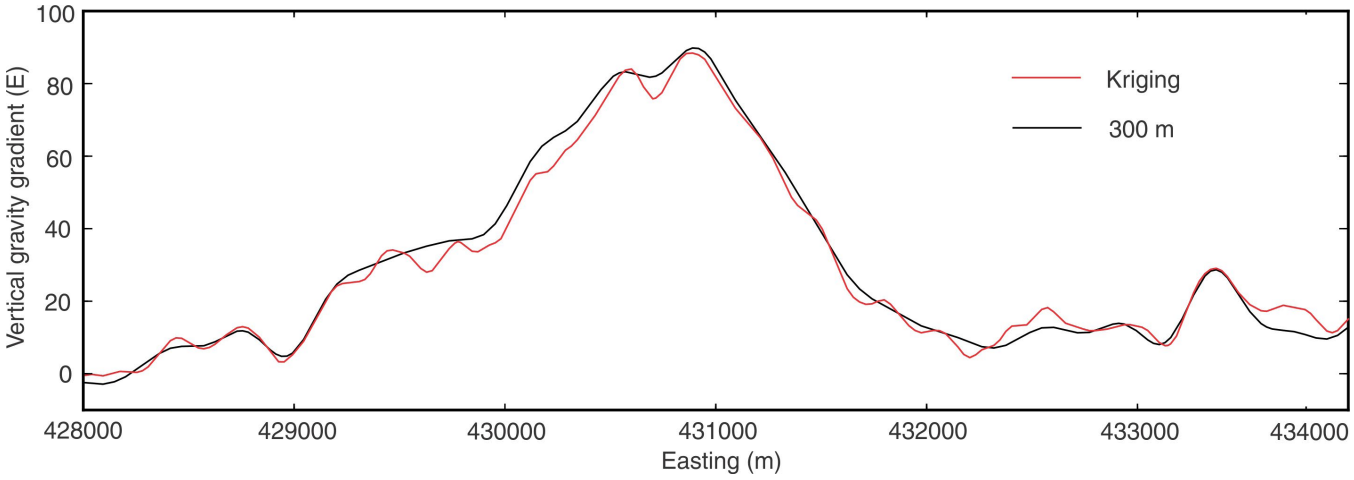


**Figure 10.** Comparison between the 300 m low-pass filtered vertical gradient of the gravity field and the vertical gradient of gravity calculated by kriging along line 11220.

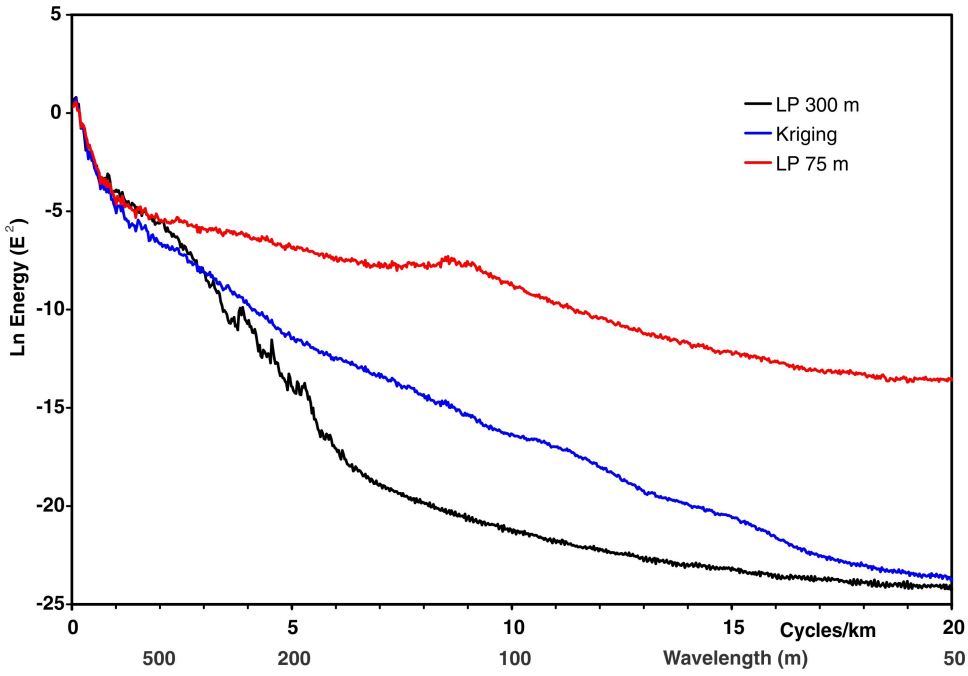


**Figure 11.** Radially averaged energy spectra of grids from the 300 m low-pass filtered data, the 75 m low-pass filtered data and grid calculated by kriging the 75 m low-pass filtered data.

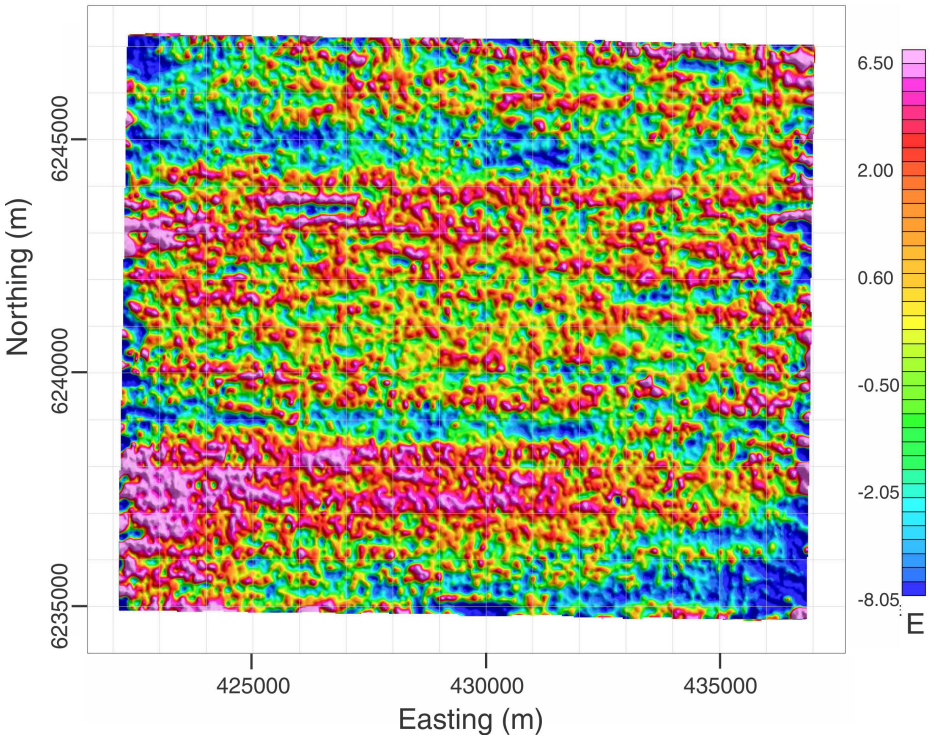


**Figure 12.** Difference between the vertical gradient grid ($G_{DD}$) calculated by kriging the 75 m low-pass filtered data and the grid calculated from the 300 m low-pass filtered data. Standard deviation of the difference grid is 3.4 E.

gravity-gradiometry data improves the across-line continuity and in some places improves resolution compared to simply interpolating the 300 m low-pass filtered data by minimum curvature. The radially averaged spectra of these two grids show that the data interpolated by kriging has more energy at mid wavelengths than the grid interpolated by minimum curvature suggesting increased information content, probably in the form of reliable geological signal. The difference seen at long wavelengths is likely due to kriging using more data points to interpolate each grid value than minimum curvature, thus providing better estimates of the interpolated values. Results from this study indicate that kriging is a better estimator of gravity-gradient values than simple low-pass filtering and minimum curvature gridding. The Strange Lake data have a low signal-to-noise ratio because most geological units in the area have very small density contrasts. It would certainly be worthwhile to repeat the study in an area where strong density contrasts exist.

## REFERENCES


Bélanger, M., 1984. Région du lac Brisson; Ministère de l'Energie et des Ressources, Québec, Open File DP 84–20, scale 1:50 000.

Blakely, R.J., 1996. Potential theory in magnetic and gravity applications; Cambridge University Press, 464 p.

Briggs, I.C., 1974. Machine contouring using minimum curvature; Geophysics, v. 39, p. 39–48. doi:10.1190/1.1440410

Chilès, J.-P. and Delfiner, P., 1999. Geostatistics: modeling spatial uncertainty; Wiley Series in probability and statistics, 687 p., <http://onlinelibrary.wiley.com/doi/10.1002/9781118136188.scard/summary> [accessed May 29, 2013]. doi:10.1002/9781118136188.scard

Deutsch, C.V. and Journel, A.G., 1992. GSLIB: Geostatistical software library and user's guide; Oxford University Press, 340 p.

Dransfield, M., 2007. Airborne gravity gradiometry in the search for mineral deposits; *in* Proceedings of Exploration 07: Fifth Decennial International Conference on Mineral Exploration, (ed.) B. Milkereit; Decennial Mineral Exploration Conferences, p. 341–354.

Dransfield, M., 2010a. Conforming Falcon gravity and the global gravity anomaly; Geophysical Prospecting, v. 58, p. 469–483. doi:10.1111/j.1365-2478.2009.00830.x

Dransfield, M., 2010b. Advances in airborne gravity gradiometry at Fugro Airborne Surveys; EGM 2010 International Workshop: Adding new value to Electromagnetic, Gravity and Magnetic Methods for Exploration Capri, Italy, April 11–14, 2010.

Dransfield, M., Christensen, A., Dioro, P., Rose, M., and Stone, P., 2001. FALCON test results from the Bathurst Mining camp: ASEG 15th Geophysical Conference and Exhibition, August 2001, Brisbane, Extended Abstracts.

Dumont, R. and Jones, A., 2012. Airborne gravity gradiometer and magnetic survey of the Strange Lake area, part of NTS 24A/8; Geological Survey of Canada, Open File 7170; Ministère des Ressources naturelles et de la Faune du Québec, DP-2012–06; Newfoundland and Labrador Department of Natural Resources, Geological Survey Open File 024A/08/0035; scale 1: 25 000. doi:10.4095/291595

Isaaks, E.H. and Srivastava, R.M., 1989. An introduction to applied geostatistics; Oxford University Press, New York, 338 p.

Kanasewich, E.R., 1981. Time sequence analysis in geophysics; University of Alberta Press, 480 p.

Miller, R., 1990. The Strange Lake pegmatite-aplite-hosted rare-metal deposit, Labrador; Current Research, Newfoundland Department of Mines and Energy, Geological Survey Branch, Report 90-4, p. 171–182.

Pillet, D., Chenevoy, M., and Bélanger, M., 1992. Pétrologie du granite peralcalin du lac Brisson, Labrador central, Nouveau-Québec. 1. Mode de mise en place et évolution chimique ; Journal canadien des sciences de la terre, v. 29, no. 2, v. 353–372.

Rainsford, D., Houlé, M.G., Metsaranta, R., Keating, P., and Pilkington, M., 2011. An overview of the McFaulds Lake airborne gravity gradiometer and magnetic survey, Northwestern Ontario; Summary of Field Work and Other Activities 2011, Ontario Geological Survey, Open File Report 6270, p. 39-1 to 39-8.



Geological Survey of Canada Project 340316NU61